



The 5th International Conference on Ambient Systems, Networks and Technologies (ANT-2014)

A model of assessment of collateral damage on power grids based on complex network theory

Gianni Fenu^{a,*}, Pier Luigi Pau^a

^aDepartment of Computer Science, University of Cagliari, Via Ospedale 72, 09124 Cagliari, Italy

Abstract

As power grids are gradually adjusted to fit into a smart grid paradigm, a common problem is to identify locations where it is most beneficial to introduce distributed generation. In order to assist in such a decision, we work on a graph model of a regional power grid, and propose a method to assess collateral damage to the network resulting from a localized failure. We perform complex network analysis on multiple instances of the network, looking for correlations between estimated damages and betweenness centrality indices, attempting to determine which model is best suited to predict features of our network.

© 2014 The Authors. Published by Elsevier B.V. This is an open access article under the CC BY-NC-ND license

(<http://creativecommons.org/licenses/by-nc-nd/3.0/>).

Selection and Peer-review under responsibility of the Program Chairs.

Keywords: Complex networks; Optimization; Power grids; Smart grids; Vulnerability analysis

1. Introduction

Electrical power transmission and distribution networks are gradually abandoning a traditional model and embracing a ‘smart grid’ paradigm. The traditional model is conceptually unidirectional, in the sense that it aims at a steady flow of power from generation sites to consumers through one or more substations. Control of a power grid generally involves operation of two co-dependent systems: the Energy Management System (EMS) and the Distribution Management System (DMS)¹. The EMS is intended to regulate energy transmission from power plants to substations, whereas the DMS is to control the distribution grid connecting substations with consumers. Several important functions happen at substations, including voltage transformation, breaking short circuits, and managing overloads.

The transition to a smart grid is desirable for multiple reasons. Among them, we mention the motivation to be prepared for the decline in availability of fossil fuels, especially as the risk associated with practices such as offshore drilling may have to be reassessed²; a need to increase the efficiency of the grid, by reducing waste of energy; and the importance of improving the reliability and robustness, for instance, implementing the best possible strategies to avoid cascading blackouts. One of the preliminary steps that make up the planning phase of this transition from a traditional power grid is a vulnerability assessment³. This activity involves estimating damage to the network delivered by the failure of specific areas or elements; this is useful to determine which parts of the network it is most pressing to improve upon, for instance, by increasing redundancy or introducing distributed generation.

* Corresponding author. Tel.: +39-070-675-8759 ; fax: +39-070-675-8504.

E-mail address: fenu@unica.it

The remainder of this work is organized as follows. In section 2, we revise the main concepts concerning smart grids. In section 3, we describe our main model of the network and how we set up an optimization problem based on it. Section 4 concerns model variants upon which we perform complex network analysis. In section 5, we describe our proposal for a measure of network damage. Section 6 presents results of experiments and the correlation of these results with those from complex network analysis. Lastly, in section 7, we draw our conclusions and set up foundations for future work.

2. The smart grid paradigm and state of the art

There exist multiple definitions of the concept of smart grids, varying according to points of view; however, a number of common points can be identified⁴. Under a smart grid model, additional infrastructure for information and communication is integrated with the electricity infrastructure⁵. Information can flow between generation sites and consumers, in both directions; moreover, consumer nodes have the ability to contribute power to the rest of the network, in the event that they have a local surplus due to local generation (e.g. solar panels) or, in a future, by discharging batteries of electrical cars or other appliances with accumulators when they are not needed⁶. Information on the state of every agent in the network is gathered, to enable an optimization of power flows, applying techniques that are suitable even as production of power is topologically distributed and entrusted to an open market⁷. A large grid can be designed as an aggregation of ‘microgrids’, which have the ability to operate in interconnected or isolated mode⁸.

Recent efforts on development of smart grids have focused on implementing an ability to detect and recover from faults, reducing length of blackout periods compared to traditional approaches⁹. It is also desirable to achieve quick reactions to changes in demand and supply, making adjustments to power flows in order to reduce energy losses and reduce risks of blackout events, and employing the best strategies to minimize voltage spikes. It is important to note that smart grids ought to be designed to withstand attacks from cyber-criminals and malicious users, which may affect the stability and reliability of operations, the availability of service, or the privacy of customers and the confidentiality of data in general¹⁰.

The transition to a smart grid paradigm requires either that a smart grid is designed from scratch, or that an existing infrastructure is upgraded according to new needs¹¹. The former approach is certainly possible, but generally not preferred because of its complexity. The latter approach, on the other hand, constitutes a slower process and requires developing a proper strategy regarding which goals take priority, as well as where it is more sensible to begin the transition.

3. Network model and optimization

As an object of study, we consider a high-level network model of the Sardinian power grid, still by large based on the traditional power grid paradigm, although smart meters have been installed for most customers and part of power generation is based on renewable sources. Our network is modeled as a directed graph $G = (V, A)$, where V is a set of vertices (nodes), each corresponding either to a power plant, or to an area where service is offered; A is a set of arcs (directed edges), representing connections between areas or from a power plant to an area. Nodes are labeled according to the category they fall into: power plant nodes, urban area nodes and industrial area nodes. Power plant nodes represent the main source of power generation, i.e. thermoelectric and hydroelectric power plants, as well as dedicated production sites based on renewable energy. Urban area nodes are associated with the consumption of a city, a conglomerate or a district; each may include one or more substations. Areas in proximity of power plants may be connected directly to a power plant nodes, while other urban areas receive power that flows from remote power plants through neighboring urban areas. Lastly, industrial area nodes represent sink nodes that aggregate the demand of industrial activities in a specific area. These nodes are always connected to one or more neighboring urban area nodes.

Power lines are modeled with arcs on the graph. Power plant nodes have only outbound arcs, and industrial area nodes have only inbound arcs; all remaining connections are modeled as pairs of arcs with opposite orientation. We refer to the complete model of our network as the *healthy state* of the network.

We consider a multiple-source, multiple-sink minimum cost flow problem on this graph model. Each arc $(u, v) \in A$ is associated with a capacity $c(u, v)$, i.e. the maximum amount of power that can flow through the arc, and a lower bound $l(u, v)$ that denotes the minimum amount that must flow on the arc. Each arc is also associated with a cost $a(u, v)$ that represents a unitary cost of power flow on that arc. The decision variables are arc flows, denoted by $f(u, v)$, where $(u, v) \in A$. Our objective function is thus

$$z = \sum_{(u,v) \in A} a(u, v) \cdot f(u, v). \quad (1)$$

Most power lines in the Sardinian power grid can be classified as 150 kV, 220 kV or 380 kV cables. Moreover, they belong to one of four categories according to their physical structure: Simple Terna Single-Circuit (500 A), Double Terna Single-Circuit (1000 A), Simple Terna Bi-Circuit (1000 A) and Simple Terna Triple-Circuit (2000 A). The maximum amount of energy that can be sent over a power line is calculated as $V \cdot A$. In our model, the value of $c(u, v)$ was determined for each arc according to the number of lines and these calculations over each line, whereas the value of $l(u, v)$ is set to 0 for every arc.

Each node $v \in V$ has a parameter $b(v) \in \mathbb{R}$ representing its aggregate supply or demand of energy. Supply is represented as positive, and demand as negative. Hence, if $b(v) < 0$ then v is a sink node, whereas if $b(v) > 0$ it is a source node (i.e. a power plant or a node where production surpasses consumption). The data needed to determine the value of $b(v)$ for each node was retrieved according to historical and statistical data by Terna (Italian leader in energy distribution). Source nodes (power plants) are associated with their maximum output in a time unit, whereas sink nodes (urban and industrial areas) are assigned a value based on an estimation of their average consumption in the same time unit, with their signed changed to negative to match our convention. Each node determines a constraint due to its balance value:

$$\forall v \in V, \sum_{(v,u) \in A} f(v, u) - \sum_{(u,v) \in A} f(u, v) = b(v). \quad (2)$$

Since optimizers work under the assumption that $\sum_{v \in V} b(v) = 0$ (supply and demand are balanced), we add an artificial node t , as well as artificial arcs from nodes representing power plants to t and from t to remaining nodes in V , and set a value for $b(t)$ such that the assumption is satisfied. Once arc weights for the rest of the network are determined, we will set $a(t, v)$ and $a(u, t)$, $\forall u, v \in V$ five orders of magnitude greater than $a(u, v)$, with $u, v \in V$, and $u, v \neq t$, so that the optimizer avoids running flow on artificial arcs, except in presence of surplus or deficit. The assignment of arc weights $a(u, v)$ shall be discussed later.

Operation of power grids has to take into account specific electrical properties and laws governing power flow¹². Although our model is high-level, and as such there is a degree of approximation involved in doing so, we opt to include additional constraints in the formulation of the optimization problem, meant to represent electrical properties. We find simple cycles of three and more nodes on the graph, disregarding edge orientation, and formulate additional constraints as follows:

$$\sum_{(u,v) \in C} d(u, v) \cdot f(u, v) = 0 \quad (3)$$

where C is the set of arcs which connect nodes comprising a cycle and, given a set orientation on the cycle (e.g. counter-clockwise), $d(u, v)$ equals +1 for arcs with that orientation, or -1 for arcs oriented against.

It is important to note that a loss of power occurs in power transmission. In our model, power loss isn't directly taken into account at transmission time, due to the limitations of linear optimization. Recall that power loss is calculated as follows:

$$P(i, j)_{loss} = I^2 R \quad (4)$$

where I is the current intensity and R is the electrical resistance. Substituting these by the corresponding expressions, i.e.

$$I = \frac{P(i, j)_{sent}}{V}, \quad R = \frac{\rho L}{A}, \quad (5)$$

we obtain:

$$P(i, j)_{loss} = \left(\frac{P(i, j)_{sent}}{V} \right)^2 \frac{\rho L}{A}, \quad (6)$$

where V is voltage, ρ is the resistivity of the material, L is line length and A is the cross sectional area of the cable. Naturally, it is in the best interest of the utility provider to minimize power losses. Since line length is dictated by geographical constraints, special care is used in adjusting the other variables, by a proper selection of the type of cables, including a choice of a material with low resistivity. As far as voltage is concerned, because of the costs associated with increasing voltage on power lines, it is a common choice to employ higher voltage for backbones, whereas for shorter distances, the cost of maintaining lines at a higher voltage may not be covered by the advantages of doing so.

We intend to use a measure of power loss as arc weights in our optimization problem. Since $P(i, j)_{loss}$ is calculated on the basis of $P(i, j)_{sent}$, and we derive an estimation of the latter from the optimization itself, a first estimation of power loss is computed based on an assumption that power flows towards each area in equal parts from each inbound arc. This estimation can be used to seed an iterative process, where consecutive runs of the optimizer compute estimated power flows, which in turn are used to compute power loss. Since some lines are modeled as symmetric pairs of arcs, we ‘lock’ the direction used in each pair at the first iteration, by assigning an artificially high cost to the arc oriented against the power flow, only within the optimizer. We verify that, with this restriction in effect, convergence of this process is achieved on the healthy state of the network.

4. Complex network analysis

To perform analysis of our grid as a complex network, we import a model of the network in its healthy state into a modified version of Cytoscape¹³, with added support for computing centrality indices in weighted networks. Our main focus is on the betweenness centrality index, which has a long history of being considered for use in vulnerability analyses¹⁴ and is still widely used for that purpose as of recently³. The betweenness centrality index is defined for a node $n \in V$ as:

$$C_b(n) = \sum_{s \neq n \neq t \in V} \frac{\sigma_{st}(n)}{\sigma_{st}} \quad (7)$$

where s and t are nodes in the network other than n , σ_{st} is the number of shortest paths from s to t , and $\sigma_{st}(n)$ is the number of shortest paths from s to t that n lies on. It expresses the ratio of shortest paths that go through a node, relative to the total number of shortest paths. The betweenness centrality index is often normalized to the number of node pairs excluding n , i.e. $\frac{(N-1)(N-2)}{2}$, where $N = |V|$. This way, the index of each node takes a value from 0 to 1. Higher values are linked to a greater importance of the corresponding element of the network, i.e. the removal of a node with high betweenness centrality has a higher impact on shortest paths in the network.

We perform our computation of betweenness centrality on two conceptual models of the network. In one model, the weight of each arc corresponds to the *cost*, as defined in the previous section. We can analyze the network based on the estimated costs used as seeds for the iterative process; in this case, we refer to results as *seed cost-based betweenness centrality* (SC-BC). If we perform analysis based on the costs obtained at the end of the iterative process, we discard the artificial costs and assign pair of arcs the same cost, based on the one calculated for the arc with positive flow. We refer to results of analysis on this instance of the network as *converged cost-based betweenness centrality* (CC-BC). In the second model, the weight of each arc corresponds to the estimated power flow.

As far as the network model based on power flow is concerned, it is to be noted that, in this model, arc weights represent a ‘strength’ of the link, as opposed to a cost. Since the definition of betweenness centrality involves a search for shortest paths on the network, arc weights ought to represent a cost; in order to reflect this, we use the reciprocal of the estimated power flow as a measure for the cost associated to arcs. To avoid division by zero errors, the few arcs with no associated power flow are artificially assigned a minimal power flow, significantly lower than any actual flow, for complex network analysis purposes only. We shall refer to the index calculated on the latter instance of the network as *flow-based betweenness centrality* (F-BC).

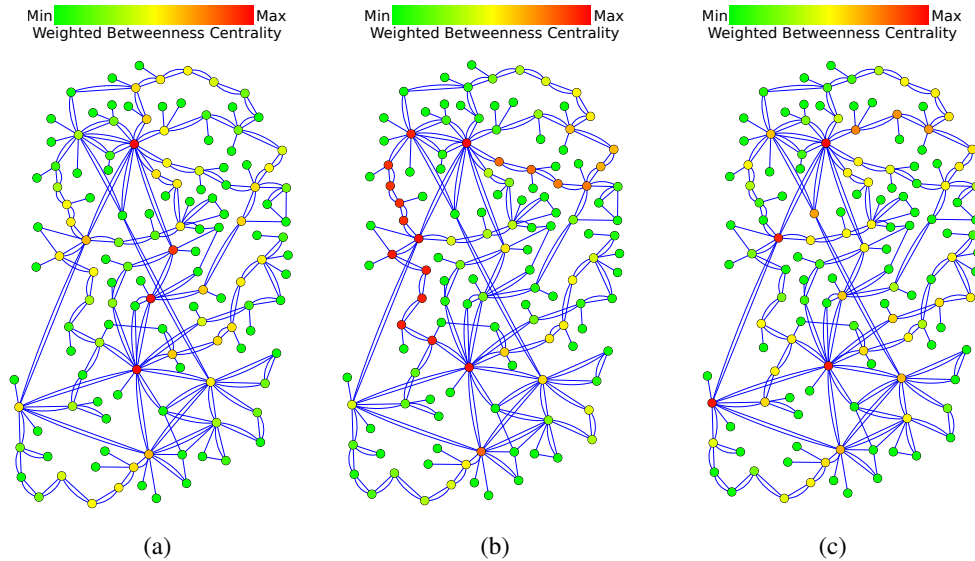


Fig. 1. Visualized analysis results for betweenness centrality. Green corresponds to the minimum value and red to the maximum value. (a) Seed cost-based. (b) Converged cost-based. (c) Flow-based.

5. Definitions

In this section, we describe the method employed to estimate collateral damage on the rest of the network as one or more nodes collapse. This method is based on comparing values of normalized objective function, obtained by solving the optimization problem discussed so far on variants of the network where certain elements have been removed.

Let $G = (V, A)$ be the complete model of the network (healthy state). Let $w \in V$ be a node that we wish to assume has failed. If detaching w and its incident arcs from G creates a disconnected component $G_d(w) = (V_d, A_d)$ on the network which has no power plant nodes, then we shall consider that the whole component is to be removed, otherwise only w is to be removed. We denote $F(w) \subset V$ as the subset of nodes in V to be removed from G , i.e. $F(w) = \{w\} \cup V_d$, where V_d may be an empty set. Lastly, let $D(w) \subset A$ be the subset of arcs in A that are incident to at least one node in $F(w)$. From this point onwards, when it is clear from the context which set is intended, we may denote $F(w)$, $D(w)$ simply as F , D for brevity.

Let $G'(w) = (V', A')$ be a modified version of G with elements from (F, D) removed, i.e.

$$V' = V \setminus F, \quad (8)$$

$$A' = A \setminus D, \quad (9)$$

and let $G''(w) = (V, A)$ be a graph model of the network including all the elements in G . We shall define optimization problems analogous to the one described in section 3 on $G'(w)$ and $G''(w)$. Let $a'(u, v)$, $b'(u)$, $c'(u, v)$ be the cost, balance and capacity values associated with elements of $G'(w)$, equal to the corresponding values $a(u, v)$, $b(u)$, $c(u, v)$ for nodes in V' and arcs in A' . As far as the problem on $G''(w)$ is concerned, we shall associate values $a''(u, v)$, $c''(u, v)$, equal to the corresponding $a(u, v)$, $c(u, v)$ from the problem on G , and $b''(u)$ defined as follows:

$$\forall u \in V, b''(u) = \begin{cases} 0 & \text{if } u \in F; \\ b(u) & \text{otherwise,} \end{cases} \quad (10)$$

i.e. the problem on an instance of G'' is identical to the one defined on G , except that the balance values for nodes in F have been set to zero. Lower capacities shall be set to zero in every instance of our optimization problems.

Let z be the value of the objective function, obtained by solving the min cost flow problem described in section 3 on G :

$$z = \sum_{(u,w) \in A} a(u,w) \cdot f(u,w) \quad (11)$$

and, likewise, let $z'(w)$, $z''(w)$ be the values of the objective functions obtained by solving the problems defined on $G'(w)$, $G''(w)$ respectively, where the set of constraints is built in the same way as in the problem for G , except that constraints for cycles including nodes in $F(w)$ defined in (3) are dropped.

The next step is to normalize values to make them comparable. Define the total demand of a network as

$$\hat{b} = - \sum_{u \in V, b(u) < 0} b(u) \quad (12)$$

and the sum of artificial costs, defined as

$$z^* = \sum_{(u,t) \in A} a(u,t) \cdot f(u,t) + \sum_{(t,u) \in A} a(t,u) \cdot f(t,u) \quad (13)$$

where t is the artificial sink node. Consider the total cost with the artificial costs removed, and normalize it to the demand on the network:

$$y = \frac{z - z^*}{\hat{b}}. \quad (14)$$

Define $\hat{b}'(w)$, $y'(w)$, $\hat{b}''(w)$, $y''(w)$ accordingly, with respect to the optimization problems defined above on $G'(w)$, $G''(w)$. Also note that it is always necessary to check whether any $f(t,u)$, $u \in V$ is above 0, i.e. if any node has a deficit or has become unreachable. We shall refer to the number of nodes with a deficit as $d(w)$.

Following these definitions, since $G'(w)$ represents the network G where node w has failed, and $G''(w)$ represents an ideal situation where G is healthy, the demand of nodes in $F(w)$ has been removed, and the cycle constraints relative to w have been ignored, it follows that $y'(w)$ and $y''(w)$ are directly comparable. Then,

$$Collateral(w) = y'(w) - y''(w) \quad (15)$$

shall be our measurement of collateral damage from the failure of w . Due to the removal of artificial costs, this figure does not capture the existence of deficit nodes in the graph; for this reason, the number of deficit nodes ought to be paired with this figure, which aims at representing how much the unavailability of paths on the network affects costs of providing service where it is still possible to do so.

The same process can be initiated assuming the failure of a set of nodes rather than a single node, i.e. choosing a $F \subset V$ directly, such that it creates no disconnected components devoid of power plant nodes. In that case, the resulting figures can be referred to as $G'(F)$, $G''(F)$, $y'(F)$, $y''(F)$, etc. Following definitions, we have that $Collateral(\emptyset) = 0$.

6. Case Study

Having calculated the flow-based and cost-based betweenness centrality index of each node, we proceed to solve the optimization problem on several modified instances of the network, in order to assess collateral damage based on the definitions of the previous section.

Each node marked as an 'urban area' is considered as a starting node. We shall label each experiment with same ID as the starting node (nodes are assigned ID numbers based on administrative references), in order to attempt to find a correlation between the results and the centrality indices calculated on each node. For each starting node v , we perform an experiment as described in the previous section, running a single instance of the optimization problem and using the initial costs. When $d(v) > 0$, we perform additional experiments building a list of failed nodes (F') which includes $F(v)$ and the nodes with deficit from the corresponding experiment. If necessary, we iterate until $d(F') = 0$. For each starting node v , we take note of the number of removed nodes in the final F' set, as well as the resulting value of $Collateral(F')$.

We consider these values and calculate Pearson correlation coefficients between the set of calculated collateral damages and the sets of betweenness centrality indices of the corresponding starting nodes. Results are found in table 1. Recall that Pearson correlation coefficients range from -1 to 1 , with values close to -1 representing inverse linear correlation, and values close to 1 corresponding to direct linear correlation. Values over 0.7 are usually considered a sign of a strong direct correlation. We observe that none of the considered indices appears to have such a strong correlation, but the index based on seed costs comes close at about 0.65 . This correlation seems to be lost when we consider converged costs, but the index from flow analysis performed on the healthy state network after cost convergence recovers some degree of correlation.

Table 1. Pearson correlation coefficients between $Collateral(F')$, for which $d(F') = 0$, built on each starting node representing an urban area, and betweenness centrality indices.

| Betweenness centrality index | Pearson correlation with Collateral |
|------------------------------|-------------------------------------|
| Seed Cost-based | 0.650460064 |
| Converged Cost-based | 0.231452099 |
| Flow-based | 0.548274258 |

As a sample, some specific results are reported in table 2. Worth noting are the experiments where a ‘hub’ node, i.e. a node denoted by a high degree, is selected as a starting node; for example, such nodes are the ones representing the urban areas of Codrongianos (ID 70) and Villasor (ID 40). Consistently with being topologically central nodes, these nodes are characterized by high values on the betweenness indices. The collateral damages associated with their failure are also among the highest. With few exceptions, collateral damage values close to 0 are found in nodes having very small betweenness centrality.

Table 2. Results of computation of $Collateral(F)$ for some F , for which $d(F) = 0$. The first column represents F . Where multiple nodes are included, the first node in the list is the one for which betweenness centralities are reported, e.g. where $F = \{21, 96\}$ the betweenness centrality of the node with ID 21 is reported.

| Removed node IDs | y' | y'' | Collateral | F-BC | CC-BC | SC-BC |
|------------------|-------------|-------------|-------------|---------|---------|---------|
| none | 40378.58499 | 40378.58499 | 0 | N/A | N/A | N/A |
| 6 | 40480.58231 | 40480.58231 | 0 | 0.00000 | 0.00000 | 0.00000 |
| 10 | 40270.57417 | 40270.57417 | 0 | 0.00619 | 0.00231 | 0.00000 |
| ... | ... | ... | ... | ... | ... | ... |
| 38 | 40378.58499 | 40378.58499 | $< 10^{-5}$ | 0.00000 | 0.00000 | 0.00000 |
| 63 | 40352.82864 | 40352.82864 | $< 10^{-5}$ | 0.01810 | 0.29389 | 0.01827 |
| 60 | 40393.82264 | 40393.73924 | 0.08340 | 0.00613 | 0.02429 | 0.01024 |
| {21, 96} | 40547.61212 | 40547.16976 | 0.44236 | 0.00630 | 0.29858 | 0.03620 |
| 20 | 40379.23947 | 40378.60582 | 0.63364 | 0.00000 | 0.02429 | 0.09195 |
| 78 | 40416.19985 | 40415.01453 | 1.18532 | 0.04551 | 0.14394 | 0.03609 |
| ... | ... | ... | ... | ... | ... | ... |
| 81 | 40474.87219 | 40389.95289 | 84.91929 | 0.03007 | 0.04638 | 0.02417 |
| 65 | 40432.29062 | 40341.52756 | 90.76306 | 0.00162 | 0.20657 | 0.00000 |
| 76 | 40439.03108 | 40348.16189 | 90.86919 | 0.01822 | 0.03533 | 0.03591 |
| ... | ... | ... | ... | ... | ... | ... |
| 64 | 40659.30957 | 40135.69493 | 523.61464 | 0.02718 | 0.02643 | 0.05748 |
| 1 | 40627.79022 | 40093.67589 | 534.11433 | 0.00000 | 0.00000 | 0.00619 |
| 70 | 40694.38290 | 39773.10907 | 921.27383 | 0.30893 | 0.04632 | 0.40802 |
| {31, 106} | 41763.85277 | 40840.63726 | 923.21551 | 0.09507 | 0.31419 | 0.01833 |
| 40 | 41211.74186 | 39633.23393 | 1578.50793 | 0.27938 | 0.33085 | 0.40204 |

7. Conclusions and future work

In this paper, we discuss a method to assess collateral damage to the network resulting from the failure of a specific node, subsystem of nodes or set of nodes, and study the correlation between these estimations of damage and betweenness centrality indices, derived by analyzing different models of the power grid using complex network theory. We find a moderate degree of correlation between seed cost-based betweenness centrality and our measure of collateral damage. Furthermore, we notice that analyzing the network model based on converged costs, flow analysis provides better correlation with collateral damage than cost analysis does. Taking this result into account, it becomes possible to favor analysis of flows in the next steps of research.

Furthermore, in order to develop a sensible path towards adding smart grid features to the existing infrastructure, we are going to experiment with extended models of the network where we add hypothetical generation based on renewable sources, in an attempt to determine the locations where it would be most beneficial to do so in the short term, especially with the goal of increasing the general reliability of the network as a whole.

Acknowledgements

Pier Luigi Pau gratefully acknowledges Sardinia Regional Government for the financial support of his PhD scholarship (P.O.R. Sardegna F.S.E. Operational Programme of the Autonomous Region of Sardinia, European Social Fund 2007-2013 - Axis IV Human Resources, Objective I.3, Line of Activity I.3.1.).

References

1. Grasberg, L., Osterlund, L.. SCADA EMS DMS-a part of the corporate IT system. In: *22nd IEEE Power Engineering Society International Conference on Power Industry Computer Applications, 2001. PICA 2001. Innovative Computing for Power - Electric Energy Meets the Market*. 2001, p. 141–147. doi:10.1109/PICA.2001.932337.
2. Skogdalen, J.E., Vinnem, J.E.. Quantitative risk analysis of oil and gas drilling, using deepwater horizon as case study. *Reliability Engineering & System Safety* 2012;**100**:58–66. doi:10.1016/j.res.2011.12.002.
3. Chen, G., Zhao, J., Dong, Z.Y., Weller, S.R.. Complex network theory based power grid vulnerability assessment from past to future. In: *9th IET International Conference on Advances in Power System Control, Operation and Management (APSCOM 2012)*. 2012, p. 1–6. doi:10.1049/cp.2012.2165.
4. Petinrin, J., Shaaban, M.. Smart power grid: Technologies and applications. In: *2012 IEEE International Conference on Power and Energy (PECon)*. 2012, p. 892–897. doi:10.1109/PECon.2012.6450343.
5. Hashmi, M., Hanninen, S., Maki, K.. Survey of smart grid concepts, architectures, and technological demonstrations worldwide. In: *2011 IEEE PES Conference on Innovative Smart Grid Technologies (ISGT Latin America)*. 2011, p. 1–7. doi:10.1109/ISGT-LA.2011.6083192.
6. Zhou, X., Lukic, S., Bhattacharya, S., Huang, A.. Design and control of grid-connected converter in bi-directional battery charger for plug-in hybrid electric vehicle application. In: *IEEE Vehicle Power and Propulsion Conference, 2009. VPPC '09*. 2009, p. 1716–1721. doi:10.1109/VPPC.2009.5289691.
7. Dimeas, A., Hatziaargyriou, N.. Agent based control of virtual power plants. In: *International Conference on Intelligent Systems Applications to Power Systems, 2007. ISAP 2007*. 2007, p. 1–6. doi:10.1109/ISAP.2007.4441671.
8. Pipattanasomporn, M., Feroze, H., Rahman, S.. Multi-agent systems in a distributed smart grid: Design and implementation. In: *Power Systems Conference and Exposition, 2009. PSCE '09. IEEE/PES*. 2009, p. 1–8. doi:10.1109/PSCE.2009.4840087.
9. Chen, C.S., Lin, C.H., Hsieh, S.C., Hsieh, W.L.. Development of smart distribution grid. In: *2013 IEEE International Symposium on Next-Generation Electronics (ISNE)*. 2013, p. 4–6. doi:10.1109/ISNE.2013.6512272.
10. Clements, S., Kirkham, H.. Cyber-security considerations for the smart grid. In: *2010 IEEE Power and Energy Society General Meeting*. 2010, p. 1–5. doi:10.1109/PES.2010.5589829.
11. Brown, R.. Impact of smart grid on distribution system design. In: *2008 IEEE Power and Energy Society General Meeting - Conversion and Delivery of Electrical Energy in the 21st Century*. 2008, p. 1–4. doi:10.1109/PES.2008.4596843.
12. Overbye, T.J.. Power system simulation: understanding small- and large-system operations. *IEEE Power and Energy Magazine* 2004;**2**(1):20–30. doi:10.1109/MPAE.2004.1263413.
13. Smoot, M.E., Ono, K., Ruschinski, J., Wang, P.L., Ideker, T.. Cytoscape 2.8: new features for data integration and network visualization. *Bioinformatics (Oxford, England)* 2011;**27**(3):431–432. doi:10.1093/bioinformatics/btq675; PMID: 21149340.
14. Albert, R., Albert, I., Nakarado, G.L.. Structural vulnerability of the north american power grid. *Physical Review E* 2004;**69**(2):025103. doi:10.1103/PhysRevE.69.025103.